J Membrane Biol (2007) 218:29–37
DOI 10.1007/s00232-007-9025-0

A Deafness-Associated Mutant Human Connexin 26 Improves the Epithelial Barrier *In Vitro*

Y. K. Stella Man · Caroline Trolove · Daniel Tattersall · Anna C. Thomas · Annie Papakonstantinopoulou · Drashnika Patel · Claire Scott · Jiehan Chong · Daniel J. Jagger · Edel A. O'Toole · Harshad Navsaria · Michael A. Curtis · David P. Kelsell

Received: 30 March 2007 / Accepted: 4 April 2007 / Published online: 21 June 2007

Abstract A large proportion of recessive nonsyndromic hearing loss is due to mutations in the *GJB2* gene encoding connexin 26 (Cx26), a component of a gap junction. Within different ethnic groups there are specific common recessive mutations, each with a relatively high carrier frequency, suggesting the possibility of heterozygous advantage. Carriers of the R143W *GJB2* allele, the most prevalent in the African population, present with a thicker epidermis than noncarriers. In this study, we show that (R143W)Cx26-expressing keratinocytes form a significantly thicker epidermis in an organotypic coculture skin model. In addition, we show increased migration of cells expressing (R143W)Cx26 compared to (WT)Cx26-overexpressing cells. We also demonstrate that cells expressing (R143W)Cx26 are significantly less susceptible to cellular invasion by the enteric pathogen *Shigella flexneri* than (WT)Cx26-expressing cells. These *in vitro* studies suggest an advantageous effect of (R143W)Cx26 in epithelial cells.

The first two authors contributed equally to this work.

Y. K. S. Man · C. Trolove · D. Tattersall · A. C. Thomas · D. Patel · C. Scott · E. A. O'Toole · H. Navsaria · D. P. Kelsell (✉)
Centre for Cutaneous Research, Institute of Cell and Molecular Science, Queen Mary University of London, 4 Newark Street, Whitechapel, London E1 2AT, United Kingdom
e-mail: d.p.kelsell@qmul.ac.uk

A. Papakonstantinopoulou · M. A. Curtis
Centre for Infectious Diseases, Institute of Cell and Molecular Science, Queen Mary University of London, Whitechapel, London E1 2AT, United Kingdom

J. Chong · D. J. Jagger
Centre for Auditory Research, UCL Ear Institute, University College London, London WC1X 8EE, United Kingdom

Keywords Connexin 26 · Deafness · Epithelial barrier

Introduction

It has been suggested that intercellular communication via gap junctions plays a role in keratinocyte differentiation and wound healing by regulating the passage of ions, small metabolites and second messenger molecules (<1 kDa) (Goliger & Paul, 1995). Specific connexins are expressed at different layers (or strata) of the normal human epidermis. One of the predominant connexins is connexin 43 (Cx43), which is expressed throughout the suprabasal layers. Extremely low levels of Cx26 are expressed in the basal layer, and similarly, Cx30 is sparsely expressed in the basal and granular layers (Di et al., 2001; Lucke et al., 1999). The expression and distribution of these epidermal connexins alter during various stages of wound healing. After wounding rat epidermis *in vivo*, Cx26 expression was upregulated in the differentiated cells proximal to the wound but downregulated in the cells at the wound edge. Using dye transfer analysis, the changes in connexin expression corresponded to changes in junctional communication (Goliger & Paul, 1995). In addition, the enteric pathogen *Shigella flexneri* can open Cx26 hemichannels, allowing release of adenosine triphosphate (Tran Van Nhieu et al., 2003), suggesting that Cx26 may play a role in bacterial cell entry.

Distinct dominant mutations in *GJB2* encoding Cx26 can produce an array of ectodermal phenotypes including hearing loss, neuropathy, hair growth abnormalities and hyperkeratosis (Richard, 2005). These disease associations support an important function for this gap junction protein in epidermal differentiation. Although dominant *GJB2* mutations can result in syndromic disease, recessive *GJB2* mutations only cause hearing loss (Kelsell et al., 1997).

Numerous studies have shown that *GJB2* mutations account for a significant proportion of recessive genetic deafness (Hutchin et al., 2005; Kenneson, Van Naarden Braun & Boyle, 2002; Snoeckx et al., 2005). Within different ethnic groups there are specific common recessive mutations that account for the majority of *GJB2*-related hearing loss, e.g., 35delG, 235delC and R143W in the European, Japanese and African populations, respectively (Brobby, Muller-Myhsok & Horstmann, 1998; Denoyelle et al., 1997; Kudo et al., 2000). Each ethnic or geographic population has a carrier frequency of 1–3%, suggesting the possibility of heterozygous advantage. Although there are no clinically defined dermatological signs, data generated from skin biopsies have shown that heterozygotes for the R143W mutation in *GJB2* have a thicker epidermis than wild-type (WT) *GJB2* homozygotes (Meyer et al., 2002). Enhanced cellular viability of HeLa cells overexpressing (R143W)Cx26 compared to those overexpressing (WT)Cx26 has also been shown (Common et al., 2004).

In this study, we demonstrate *in vitro* an extended keratinocyte differentiation program and increased migration of (R143W)Cx26-expressing cells compared to the WT counterpart. We also demonstrate that HeLa cells expressing this Cx26 mutant do not increase cellular invasion by the enteric pathogen *S. flexneri*, unlike (WT)Cx26-expressing cells.

Materials and Methods

All reagents were from Sigma (Poole, UK) unless otherwise stated.

Antibodies

Monoclonal keratin 10 (LH2), involucrin (Sy5), keratin 14 (LL002), keratin 6 (LHK6) and keratin 16 (LL025) antibodies were all generated by Cancer Research UK (CRUK). Transglutaminase 1 (TG1) (Biogenesis, Dorset, UK), keratin 2e (Abcam, Cambridge, UK), loricrin (Covance Research Products, Princeton, NJ) and Ki67 (Dako, High Wycombe, UK) antibodies were obtained commercially.

Plasmid Constructs

Full-length cDNA of (WT)Cx26, (R143W)Cx26, (WT)Cx30 and (WT)Cx31 fused with enhanced green fluorescent protein (EGFP), together with EGFP alone, was cloned and inserted into pSIN retroviral vector (Deng, Lin & Khavari, 1997). All clones were verified by automated sequencing using ABI 3700 (Genome Centre, Queen Mary University, London, UK).

Culture of nTERT Keratinocytes and HeLa Cells

The human cell line nTERT was derived from primary keratinocytes immortalized by telomerase (Dickson et al., 2000). The culture medium consisted of E4 Ham's medium containing 10% (v/v) fetal calf serum, 2 mM glutamine, 1% (v/v) RM + supplement (final concentration of 400 ng/ml hydrocortisone, 5 μg/ml insulin, 10 ng/ml Epidermal Growth Factor (EGF), 8.4 ng/ml cholera toxin, 5 μg/ml transferrin, 13 ng/ml lyothyronine), 50 units/ml penicillin-G and 50 μg/ml streptomycin sulfate. HeLa cells (ATCC, Rockville, MD) were cultured in Dulbecco's modified Eagle medium (DMEM) containing 10% (v/v) fetal calf serum, 2 mM glutamine, 50 units/ml penicillin-G and 50 μg/ml streptomycin sulfate.

Retroviral Transduction

A retroviral transduction protocol was carried out in order to create nTERT or HeLa cells that overexpress (WT)Cx26-EGFP, (R143W)Cx26-EGFP, (WT)Cx30-EGFP, (WT)Cx31-EGFP or EGFP alone. Phoenix 293 viral packaging cells were cultured in DMEM as described above. They were transfected with the plasmid constructs using a 1:3 ratio of DNA:Fugene 6 reagent (Roche, Lewes, UK). After 24 h, cells were selected with 1 μg/ml puromycin for 48 h at 37°C. The medium was replaced, and the cells were incubated at 32°C for 24 h before the virus-containing supernatant was collected, filter-sterilized and snap-frozen in liquid nitrogen. All retrovirus collections were stored at –80°C until ready for use.

For retroviral transduction, the virus was prepared in a glass container where 5 μg/ml (final concentration) polybrene reagent was added and incubated at room temperature for 15 min. Keratinocytes were also treated with polybrene by adding a final concentration of 5 μg/ml to the normal culture medium. These cells were transferred to 37°C. After 15-min incubation, the polybrene-containing medium was replaced with polybrene-treated virus. Cells were centrifuged at 350 x *g* at 32°C for 1 h. Upon completion of the centrifugation step, the virus was replaced with fresh normal culture medium and returned to 37°C/10% CO_2. After 24–48 h, cells were viewed under an ultraviolet lamp microscope to confirm expression. In all cases, transduction efficiency was comparable between constructs.

Connexin Localization

Transduced nTERT cells were plated onto coverslips at a suitable density and, after 24 h, fixed in 4% paraformaldehyde in phosphate-buffered saline (PBS) for 30 min. The cells were washed in PBS and mounted using Immu-Mount

(Thermo Electron, Waltham, MA) containing 10 μg/ml 4′,6-diamidino-2-phenylindole (DAPI), before being visualized by laser scanning confocal microscopy (LSM510; Carl Zeiss, Oberkochen, Germany).

Organotypic Coculture

Organotypic coculture was carried out following the protocol described by Ojeh, Frame & Navsaria (2001).

Dye Injection

The growing epidermis was removed from the dermis raft using fine forceps and suspended in low-melting point agarose. Small blocks of tissue in agarose were mounted on a vibratome, and sections were cut at 200 μm. Lucifer yellow (LY, 4% in 3 M LiCl) was microinjected into cells using microelectrodes with resistance ~100 MΩ. Following LY injection, slices were fixed in 4% paraformaldehyde in PBS for 30 min. Slices were then permeabilized (0.1% Triton-X) and blocked (10% normal goat serum) and subsequently incubated in an anti-LY antibody overnight at 4°C. Following several washes in PBS, the anti-LY antibody was detected using an anti-rabbit fluorescein isothiocyanate-conjugated secondary antibody. Slices were mounted in an antifade medium containing DAPI (Vectashield; Vector Laboratories, Burlingame, CA). Immunofluorescence was detected by laser scanning confocal microscopy (LSM510, Carl Zeiss). The number of cells containing LY was determined for each injection site. Data from tissue transfected with (WT)Cx26 were compared to those from (R143W)Cx26-transfected tissue using Student's unpaired *t*-test (Prism v4; Graphpad Software, San Diego, CA).

Coculture Staining

Each tissue was cut in half such that one-half was snap-frozen while embedded in Cryo-M-Bed^{TM} (Bright, Huntingdon, UK) and stored at –80°C. The other half was fixed in 4% (v/v) paraformaldehyde and embedded in paraffin. Sections were cut at 5–6 μm thickness.

Hematoxylin and Eosin Staining

Hematoxylin and eosin staining was performed on the paraffin sections following the standard protocol. Briefly, sections were dewaxed in xylene and rehydrated in sequential washes of 100%, 90% and 70% alcohol. Sections were stained in hematoxylin for 3 min, followed by eosin for 2 min, then dehydrated in 70%, 90% and 100% alcohol and mounted with DePeX (VWR, Chicago, IL).

The thickness of the cornified envelope and the epidermal/dermal junctions were measured across three representative areas of three independent sections per sample. This was repeated for three independently grown organotypic cocultures.

Immunofluorescent Staining

Frozen sections were air-dried for 30 min, and cells were permeabilized in 0.1% (v/v) Triton X–100 in PBS for 15 min. Sections were washed in PBS, blocked in 0.2 % (v/v) gelatin from cold water fish skin for 15 min and incubated with primary antibody for 1 h. All antibodies mentioned were used at a 1/200 dilution. After three PBS washes, fluorescent secondary antibody (donkey anti-rabbit or donkey anti-mouse Alexa Fluor 568; Molecular Probes, Eugene, OR) was added at a 1/1,000 dilution and incubated for 1 h protected from light exposure. Sections were washed three times in PBS, incubated with DAPI (0.125 μg/ml) for 5 min and washed three more times. Sections were mounted with immunomount reagent (ThermoShandon, Pittsburgh, PA) and viewed under a Nikon (Tokyo, Japan) Eclipse TE2000-S microscope.

Scratch Migration Assay

Cells were seeded at 5 x 10^5 per well in six-well culture dishes. Each cell sample was seeded in duplicate and incubated at 37°C for 24 h. After culturing in serum-free medium (Ham's DMEM) for 24 h, cells were treated with mitomycin C at 10 mg/ml for 1 h at 37°C to inhibit proliferation. The medium was removed and a ''cross'' scratched across the dish using a P1000 pipette tip, leaving ''scratched'' areas with no cells (Boyer et al., 1989). Cells were washed three times in PBS. An area of the ''cross'' was imaged at x5 magnification at 0 and 48 h after the initial scratch to ensure the same part of the scratch was imaged each time. Cells were incubated at 37°C/5% CO_2 in between time points. Images were analyzed using the ImageJ software program (available at http://www.rsb.info.nih.gov/ij/) whereby the cell-free area was recorded at each time point. The data are presented as average percentage area migrated.

Proliferation Assay

Cellular proliferation was analyzed using the alamar blue assay (Biosource, Camarillo, CA). Cells (1 x 10^4) were seeded in triplicate in 12-well plates and incubated for 20 h at 37°C to allow them to attach to the culture dish. Cells were washed with PBS, and 10% (v/v) alamar blue dye in normal culture medium was added. Cells were incubated

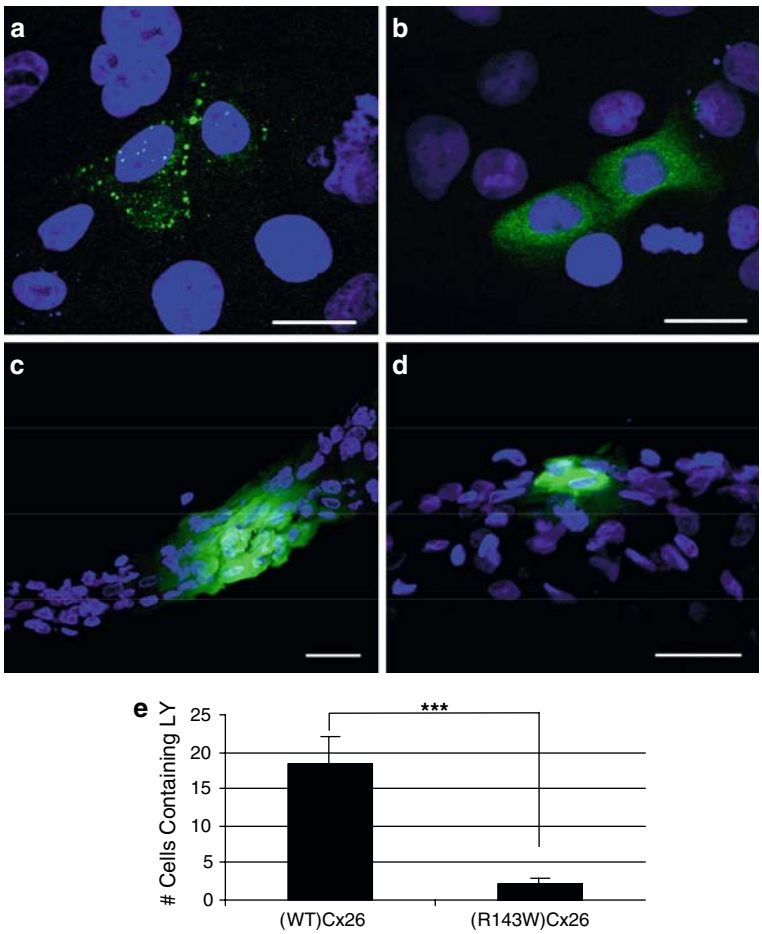

Fig. 1 Localization of (WT)Cx26 (**a**) and (R143W)Cx26 (**b**) (*green*). Note the aggregations of (WT)Cx26 at the cell periphery, which are indicative of gap junction plaques, are absent in the cells expressing (R143W)Cx26. LY (*green*) transfer following microinjection of organotypic cocultures expressing (WT)Cx26 (**c**) or (R143W)Cx26 (**d**). Quantification of cells containing LY after microinjection of (WT)Cx26- and (R143W)Cx26-expressing cocultures (**e**). There is a statistical difference between the two (***$p < 0.0001$, unpaired *t*-test). (**a-d**) Scale bars = 20 μm. Nuclei are shown with blue DAPI staining

for 6 h at 37°C. For fluorescence detection, 150 μl from each sample was removed from each well, and the remaining dye was washed from the cells before normal culture medium was replaced. The assay was performed over 3 consecutive days, with fresh alamar blue added 6 h prior to assay.

Each sample was measured in duplicate by recording the optical density at 570 nm (OD_{570}). The fold change (i.e., average OD_{570} each day/average OD_{570} on day 1) per sample was calculated and plotted against time (days).

Bacterial Invasion Assay

S. flexneri serotype 2a (2457T, ATCC) was grown in LB broth overnight at 37°C in an orbital shaker. The optical density of the culture was measured at 600 nm. Retrovirally transduced HeLa cells were seeded into 24-well dishes at 2 x 10^5 per well. The medium was removed and replaced with antibiotic-free DMEM containing 10% (v/v) fetal calf serum and 2 mM glutamine. *S. flexneri* was added to each well of transduced HeLa cells (0.93 OD_{600} units per well, corresponding to 3 x 10^7 colony-forming units). The plate was centrifuged at 15 x *g* for 2 min and incubated at 37°C/10% CO_2 for 4 h. Cells were washed three times with PBS, and medium was added containing 50 μg/ml of gentamycin and incubated at 37°C for 1 h. Following three washes in PBS, cells were lysed with 0.1% (v/v) Triton X-100 in PBS. Lysates were serially diluted in PBS and plated onto LB agar. Bacteria were propagated overnight at 37°C. Colonies were counted, and statistical analysis was carried out using a two-tailed, unpaired *t*-test.

Statistical Analysis

All statistical analyses were carried out either as a one- or a two-tailed, unpaired *t*-test, as stated, depending on the type of experiment performed. $p \leq 0.05$ was considered statistically significant.

Results

To confirm expression of the EGFP-tagged connexin proteins, cells transduced with the constructs were first visualized by confocal microscopy (Fig. 1). Aggregations were observed in cells transduced with (WT)Cx26 at the cell periphery, which are indicative of gap junction plaques. No such aggregations were observed in (R143W)Cx26-

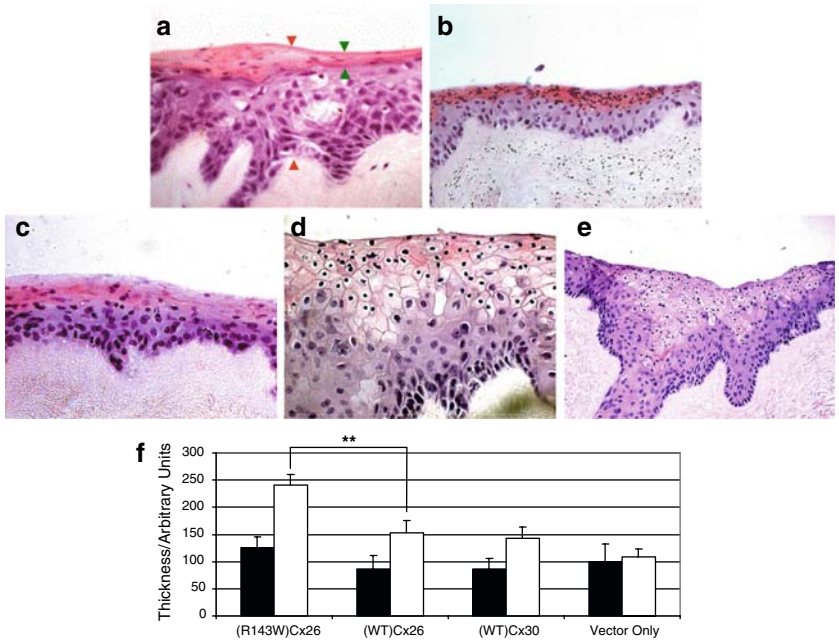

Fig. 2 Histological features of organotypic cocultures. Hematoxylin and eosin-stained sections of (**a**) pSIN-GFP (vector-only), (**b**) (WT)Cx30, (**c**) (WT)Cx26, (**d**) (R143W)Cx26 cocultures at x400 magnification and (**e**) (R143W)Cx26 at x200 magnification. *Green* and *orange arrows* in **a** represent the distance at which the eosin-positive layer and full thickness of the epidermal equivalent were measured, respectively. (**f**) Graph representing the average thickness of the eosin-positive layer (*black bars*) and average full thickness of the epidermal equivalent (*white bars*). Unpaired, two-tailed *t*-test showed that the total thickness of the epidermal equivalent of the (R143W)Cx26 coculture was statistically different from (WT)Cx26 (**$p < 0.01$). Error bars represent the standard error of the mean, $n = 3$

expressing cells. Organotypic cocultures expressing (WT)Cx26 or (R143W)Cx26 were subjected to LY dye transfer assays. While (WT)Cx26 allowed dye transfer to adjoining cells, in the (R143W)Cx26 cocultures the amount of dye transfer was significantly reduced by eightfold.

Morphological Characterization of Organotypic Cocultures Overexpressing Connexins

The morphological characteristics of keratinocytes on a three-dimensional basis were examined by organotypic cocultures (Ojeh et al., 2001). Hematoxylin and eosin staining showed little difference between the cocultures using cells transduced with (WT)Cx26-EGFP, (WT)Cx30-EGFP and pSIN-EGFP (vector-only) (Fig. 2a-c). These cocultures all exhibited typical histological features of stratified squamous epidermis, i.e., nucleated basal cells eventually differentiating into flatter, anucleated cells toward the top of the epidermal layer. (R143W)Cx26 cocultures showed evidence of a significantly thicker epidermis compared to the other samples despite there being equal numbers of keratinocytes seeded at the start of each organotypic coculture (Fig. 2d,e). Observationally, the (R143W)Cx26 coculture had more densely packed basal keratinocytes compared to the control, suggesting an increased number of proliferative cells. Some suprabasal keratinocytes in the spinous layer appeared larger, and an eosin-positive layer (stained pink) was also visible. In the latter, some cells appeared to lose their nuclei, while others retained very small nuclei. The (R143W) coculture lacked a clearly defined cornified envelope at day 14 compared to control cocultures, where it had formed by this stage. However, the (R143W) cocultures formed a cornified envelope by day 16 (*data not shown*), indicating delayed terminal differentiation.

The average epidermal thickness measurement of (R143W)Cx26 was 1.6 times higher than that corresponding to the (WT)Cx26 cocultures ($p = 0.003$) (Fig. 2f). The average measurements of the eosin-positive (pink) layer remained fairly constant in all the cocultures. Similarly, no differences in the epidermal thickness measurements were found between (WT)Cx26 and (WT)Cx30 cocultures compared to the vector-only control. These data are comparable to *in vivo* results (Meyer et al., 2002).

Immunohistochemistry was performed to assess any molecular changes in the differentiation program of the transduced keratinocytes on organotypic cocultures using differentiation markers. Normal expression patterns were found for keratin 10, TG1, involucrin, keratin 2e and loricrin between all cocultures (*data not shown*). This suggests that the onset of late differentiation is similar between all the organotypic models. In contrast, a larger number of keratin 14-positive cells was observed in (R143W)Cx26 cocultures compared to the other cocultures

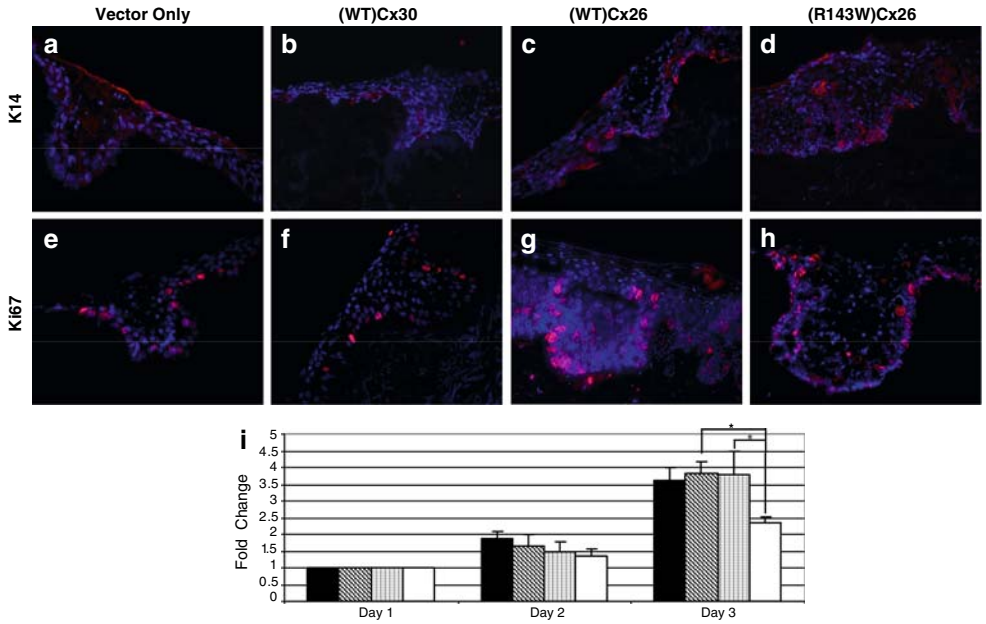

Fig. 3 Characterization of nTERTs overexpressing (WT)Cx26, (WT)Cx30 and (R143W)Cx26. Keratin 14 immunofluorescent staining (*red*) of (**a**) vector-only control, (**b**) (WT)Cx30, (**c**) (WT)Cx26 and (**d**) (R143W)Cx26 cocultures. Ki67 immunofluorescence (*red*) of (**e**) vector-only control, (**f**) (WT)Cx30, (**g**) (WT)Cx26 and (**h**) (R143W)Cx26 cocultures. Nuclei are shown with *blue* DAPI staining. (**i**) Graph showing the average fold change in proliferation over a 3-day time course. *Black, striped, speckled* and *white bars* represent nTERTS overexpressing (R143W)Cx26, (WT)Cx26, (WT)Cx30 and vector-only control, respectively. The data represent mean ± standard error of the mean ($n = 3$). *$p \leq 0.05$

(Fig. 3a-d). Keratin 14, a basal cell marker of the epidermis, was not only expressed in the basal layer but was also evident in (R143W)Cx26-expressing cells in the higher layers of the three-dimensional culture.

Proliferative Features of Organotypic Cocultures and nTERT Keratinocytes

No evidence of hyperproliferation was observed, with only weak staining of keratin 6 and keratin 16 observed in all cocultures (*data not shown*). The proliferation status was further assessed by the cellular pattern of Ki67 expression in the organotypic cocultures (Fig. 3e-h). Ki67 is expressed in the nuclei of actively proliferating cells normally exclusive to those in the basal layer of the epidermis. This expression pattern was observed in the (WT)Cx30 culture (Fig. 3f) and in the vector-only control (Fig. 3e). More Ki67-positive keratinocytes were present along the basal layer of the (R143W)Cx26 coculture (Fig. 3h) compared to the vector-only control. Similarly, in (WT)Cx26 cocultures, Ki67 was present at an increased level in the basal layer relative to control cocultures. These Ki67-positive cells also appeared in the early spinous layer (Fig. 3g). The increase in number of proliferating (Ki67-expressing) cells in the (WT)Cx26 and (R143W)Cx26 organotypic cocultures was confirmed by a blind scoring analysis (*data not shown*). The proliferative status of the cells was also analyzed using the alamar blue assay (Fig. 3i). The data revealed that keratinocytes overexpressing (R143W)Cx26, (WT)Cx26 and (WT)Cx30 proliferated faster than the vector-only control. There was no difference in proliferation between (R143W)Cx26 and (WT)Cx26 transduced cells.

Migratory Characteristics of Keratinocytes

A scratch assay was performed to assess cell migration (Fig. 4). Keratinocytes overexpressing (R143W)Cx26 showed an increase in migration by 1.5-fold compared to the (WT)Cx26 equivalent ($p = 0.025$). (WT)Cx26 and (WT)Cx30 cells exhibited increased migration compared to vector-only control by 3.5-fold ($p = 0.0013$) and 2.7-fold ($p = 0.013$), respectively.

The Increase in Bacterial Invasion Seen in (WT)Cx26-Expressing HeLa Cells Is not Seen in the (R143W)Cx26 Counterpart

Previously, it was shown that cellular invasion of the gut pathogen *S. flexneri* is associated with opening Cx26 hemichannels in an actin-phospholipase C-dependent manner (Tran Van Nhieu et al., 2003). We have confirmed and extended these findings (Fig. 5). The total number of *S. flexneri* bacteria which invaded (WT)Cx26-overexpressing

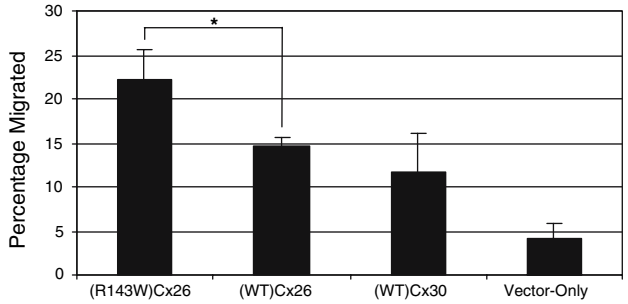

Fig. 4 Keratinocyte cellular migration analysis. A monolayer of nTERTS overexpressing (R143W)Cx26, (WT)Cx26, (WT)Cx30 or vector-only control was scratched. Graph shows the percentage of cells migrated after 48 h. The data represent mean ± standard error of the mean. Comparison was carried out using unpaired, one-tailed *t*-test where a significant difference was found between (WT)Cx26 and (R143W)Cx26. *$p \leq 0.05$

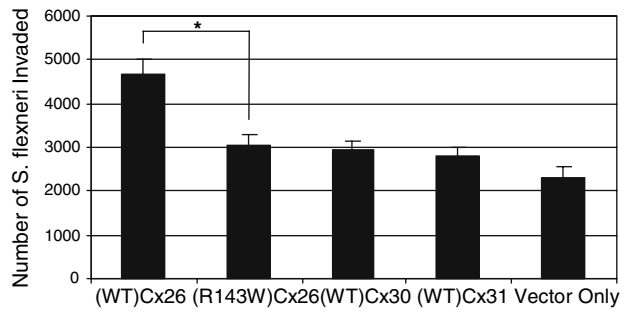

Fig. 5 Bacterial invasion via Cx26 hemichannels. Histogram showing invasion of *S. flexneri* bacteria in HeLa cells overexpressing (WT)Cx26, (R143W)Cx26, (WT)Cx30, (WT)Cx31 and vector-only control. The data represent mean ± standard error of the mean, $n = 15$. Comparison was carried out using unpaired, two-tailed *t*-test where a significant difference was found between (WT)Cx26 and (R143W)Cx26. *$p \leq 0.05$

HeLa cells was higher than in cells expressing vector-only control. Interestingly, two other epidermally expressed connexins, (WT)Cx30 and (WT)Cx31, showed no evidence for enhancing the potential for *S. flexneri* to invade. HeLa cells expressing (R143W)Cx26 do not have the increased levels of bacterial invasion observed in (WT)Cx26 transduced cells (4,670 ± 324.8 bacteria invaded in [WT]Cx26, and 3,069 ± 238.3 bacteria invaded in [R143W]Cx26). A significant difference ($p = 0.044$) in bacterial invasion was illustrated between (R143W)Cx26 and (WT)Cx26.

Discussion

Multiple differences were observed between keratinocytes overexpressing human (WT)Cx26 and those overexpressing (R143W)Cx26. (WT)Cx26 formed aggregates indicative of gap junction plaques, whereas cells expressing (R143W)Cx26 were devoid of plaque formation. Palmada et al. (2006) observed the (R143W)Cx26 mutant in the 10,000 x *g* pellet, which is consistent with an internal membranous structure. However, other studies (Wang et al., 2003) report a plasma membrane localization. Differences in cell type and expression conditions could explain these contrasting results. However, regardless of the mutant protein's cellular localization, our dye conductance experiments herein confirm that (R143W)Cx26 is unable to form functional channels (Mese et al., 2004; Palmada et al., 2006). The dye transfer observed was most likely due to endogenous nTERT connexin expression.

The human (R143W)Cx26 model presented with thickening of the epidermal equivalent, increased number of cells expressing basal marker K14 and increased cellular mobility. Coincidentally, the overall increase in thickness was similar in both our model and an *in vivo* study (Meyer et al., 2002). This might suggest that there is a limit to the overall thickness of the epidermis before it becomes pathological. Furthermore, we provide evidence that, unlike (WT)Cx26, (R143W)Cx26 did not increase *S. flexneri* invasion.

From our data in this study, the increase in cell numbers seen in the (R143W)Cx26 organotypic coculture showed little difference in proliferation compared to (WT)Cx26 cocultures, a conclusion further confirmed by the proliferation assay. Since increased proliferation cannot explain the thickened epidermis in (R143W)Cx26 cocultures, the phenotypic effect may be due to an increased number of undifferentiated basal cells, as demonstrated by the Ki67 and K14 immunostaining data, respectively. It is possible that the overall proliferation rate is unaltered but, because more undifferentiated cells are present, more daughter cells are generated, giving rise to epidermal thickening.

Additionally, skin-thickening conditions such as psoriasis and palmoplantar keratoderma display an increase in K6 and K16 expression, markers of hyperproliferation (Leigh et al., 1995). Although the organotypic coculture model of (R143W)Cx26 showed significant epidermal thickening, no significant changes were seen in K6 expression compared to the control, supporting the notion that the phenotype is not associated with any pathological changes. The very weak staining observed in all the cocultures is most likely due to the keratinocytes adopting a slight hyperproliferative state, a finding consistent with previous descriptions of organotypic cocultures (Stark et al., 2004). If the observations were not of a pathological nature, (R143W)Cx26 may exert beneficial properties to the skin.

One way R143W(Cx26) may benefit the skin is by decreasing the ability of bacterial pathogens to invade. As a preliminary experimental model we used the gut-invading pathogen *S. flexneri* in HeLa cells as HeLa cells express low endogenous levels of connexins and were previously

used to show that Cx26 enhances *S. flexneri* invasion (Trans Van Nhieu et al., 2003). Our data show that two other epidermally expressed connexins, Cx30 and Cx31, do not have a similar effect. The mechanism behind the relative specificity of Cx26 to elicit the invasion increase is yet to be explored. (R143W)Cx26-expressing cells showed reduced bacterial invasion compared with (WT)Cx26-expressing cells. This may be due to the functional disruption of the Cx26 hemichannel since the WT hemichannel is reported to allow *S. flexneri* invasion through the actin-phospholipase C-dependent pathway in HeLa cells (Tran Van Nhieu et al., 2003). Patients who carry the (R143W)Cx26 variant have increased levels of sodium and chloride in their eccrine sweat glands compared to normal individuals. This physiological finding was postulated to create an osmotic environment that is difficult for microbial colonization (Meyer et al., 2002). Our model shows that (R143W)Cx26-expressing cells are protected against this gut pathogen compared to their (WT)Cx26 counterpart. It could be possible that a similar effect is seen in keratinocytes expressing (R134W)Cx26. It is interesting to note that Cx26 expression is limited to the basal layer in interfollicular human epidermis and to the epidermal eccrine sweat glands. This specific cellular localization of Cx26 is consistent with protecting the epidermis from bacterial infection. Similarly, in human colon tissue, Cx26 expression levels appeared to be greatest around the goblet cells, cells that interact closely with the contents (bacterial or otherwise) of the gut (*data not shown*).

In human cutaneous wounding, Cx26 is expressed 24–48 h postinjury. It is detected near the wound margin, and eventually, as the wound heals, normal low expression of Cx26 resumes (Brandner et al., 2004). The role of this connexin at times of injury remains elusive. It has been suggested that Cx26 (and Cx30) is massively upregulated in psoriasis to control differentiation (Labarthe et al., 1998; Rivas et al., 1997; Wiszniewski et al., 2000). However, we did not observe any obvious differentiation changes in our Cx26 overexpression model. We postulate that Cx26 regulates the wound healing process, not by promoting it but by controlling and maybe even dampening it. Our data demonstrated that overexpression of (WT)Cx26 did not promote an increase in migration whereas inhibition of Cx26 (by the R143W mutation) appeared to lead to an effect on keratinocyte migration. In support of our hypothesis, an *in vivo* study in human skin has shown upregulation of Cx26 and Cx30 at margins of nonhealing wounds, whereas during spontaneous wound repair these connexins are absent at the leading edge of the regenerating epidermis but overexpressed behind the wound margin (Brandner et al., 2004). This expression pattern may reflect the proliferative capacity of Cx26-expressing cells, which correlates well with our study. It has been reported that cells at this location relative to the wound undergo a proliferative burst, which possibly provides a pool of extra cells to replace those lost during injury (Hertle et al., 1992; Matoltsy & Viziam, 1970).

While this report was in preparation, Segre and colleagues reported that transgenic mice heterozygous for involucrin-Cx26 had persistent Cx26 expression in the epidermis (Djalilian et al., 2006). The wounded epidermis was infiltrated with immune cells, and the wound remained in a hyperproliferative state with the remodeling phase blocked, resulting in wound healing failure. These *in vivo* data are consistent with our findings and support the hypothesis that Cx26 suppresses wound healing. In summary, these results suggest that a nonfunctional Cx26 channel due to a *GJB2* hearing loss-associated mutation confers beneficial properties to the epidermis and possibly other Cx26-expressing epithelium, resulting in an improved barrier, accelerated wound repair and protection from infection. As also recently suggested (Djalilian et al., 2006), knockdown of Cx26 expression may have a therapeutic application in wound healing and as an anti-infective.

Acknowledgements This work was funded by the Research Advisory Board of Barts and the London, the Biotechnology and Biological Sciences Research Council (BBSRC) and the Wellcome Trust to D. P. K. We express special thanks to Dr. Jash Vyas for advice and help with the migration assays and Professor Tom MacDonald for the normal human colon and help with interpretation of Cx26 localization.

References

Boyer B, Tucker GC, Valles AM, Franke WW, Thiery JP (1989) Rearrangements of desmosomal and cytoskeletal proteins during the transition from epithelial to fibroblastoid organization in cultured rat bladder carcinoma cells. J Cell Biol 109:1495–1509

Brandner JM, Houdek P, Husing B, Kaiser C, Moll I (2004) Connexins 26, 30, and 43: differences among spontaneous, chronic, and accelerated human wound healing. J Invest Dermatol 122:1310–1320

Brobby GW, Muller-Myhsok B, Horstmann RD (1998) Connexin 26 R143W mutation associated with recessive nonsyndromic sensorineural deafness in Africa [letter]. N Engl J Med 338:548–550

Common JE, Di WL, Davies D, Kelsell DP (2004) Further evidence for heterozygote advantage of GJB2 deafness mutations: a link with cell survival. J Med Genet 41:573–575

Deng H, Lin Q, Khavari PA (1997) Sustainable cutaneous gene delivery. Nat Biotechnol 15:1388–1391

Denoyelle F, Weil D, Maw MA, et al. (1997) Prelingual deafness: high prevalence of a 30delG mutation in the connexin 26 gene. Hum Mol Genet 6:2173–2177

Di WL, Rugg EL, Leigh IM, Kelsell DP (2001) Multiple epidermal connexins are expressed in different keratinocyte subpopulations including connexin 31. J Invest Dermatol 117:958–964

Dickson MA, Hahn WC, Ino Y, Ronfard V, Wu JY, Weinberg RA, Louis DN, Li FP, Rheinwald JG (2000) Human keratinocytes that express hTERT and also bypass a p16(INK4a)-enforced mechanism that limits life span become immortal yet retain normal growth and differentiation characteristics. Mol Cell Biol 20:1436–1447

Djalilian AR, McGaughey D, Patel S, Seo EY, Yang C, Cheng J, Tomic M, Sinha S, Ishida-Yamamoto A, Segre JA (2006) Connexin 26 regulates epidermal barrier and wound remodeling and promotes psoriasiform response. J Clin Invest 116:1243–1253

Goliger JA, Paul DL (1995) Wounding alters epidermal connexin expression and gap junction-mediated intercellular communication. Mol Biol Cell 6:1491–1501

Hertle M, Kubler M-D, Leigh IM, Watt FM (1992) Aberrant integrin expression during epidermal wound healing and in psoriatic epidermis. J Clin Invest 89:1892–1901

Hutchin T, Coy NN, Conlon H, Telford E, Bromelow K, Blaydon D, Taylor G, Coghill E, Brown S, Trembath R, Liu XZ, Bitner-Glindzicz M, Mueller R (2005) Assessment of the genetic causes of recessive childhood non-syndromic deafness in the UK – implications for genetic testing. Clin Genet 68:506–512

Kelsell DP, Dunlop J, Stevens HP, Lench NJ, Liang JN, Parry G, Mueller RF, Leigh IM (1997) Connexin 26 mutations in hereditary non-syndromic sensorineural deafness. Nature 387:80–83

Kenneson A, Van Naarden Braun K, Boyle C (2002) GJB2 (connexin 26) variants and nonsyndromic sensorineural hearing loss: a HuGE review. Genet Med 4:258–274

Kudo T, Ikeda K, Kure S, Matsubara Y, Oshima T, Watanabe K, Kawase T, Narisawa K, Takasaka T (2000) Novel mutations in the connexin 26 gene (*GJB2*) responsible for childhood deafness in the Japanese population. Am J Med Genet 90:141–145

Labarthe MP, Bosco D, Saurat JH, Meda P, Salomon D (1998) Upregulation of connexin 26 between keratinocytes of psoriatic lesions. J Invest Dermatol 111:72–76

Leigh IM, Navsaria H, Purkis PE, McKay IA, Bowden PE, Riddle PN (1995) Keratins (K16 and K17) as markers of keratinocyte hyperproliferation in psoriasis in vivo and in vitro. Br J Dermatol 133:501–511

Lucke T, Choudhry R, Thom R, Selmer IS, Burden AD, Hodgins MB (1999) Upregulation of connexin 26 is a feature of keratinocyte differentiation in hyperproliferative epidermis, vaginal epithelium, and buccal epithelium. J Invest Dermatol 112:354–361

Matoltsy AG, Viziam CB (1970) Further observations on epithelialization of small wounds: an autoradiographic study of incorporation and distribution of ^{3}H-thymidine in the epithelium covering skin wounds. J Invest Dermatol 55:20–25

Mese G, Londin E, Mui R, Brink PR, White TW (2004) Altered gating properties of functional Cx26 mutants associated with recessive non-syndromic hearing loss. Hum Genet 115:191–199

Meyer CG, Amedofu GK, Brandner JM, Pohland D, Timmann C, Horstmann RD (2002) Selection for deafness? Nat Med 8:1332–1333

Ojeh NO, Frame JD, Navsaria HA (2001) In vitro characterization of an artificial dermal scaffold. Tissue Eng 7:457–472

Palmada M, Schmalisch K, Bohmer C, Schug N, Pfister M, Lang F, Blin N (2006) Loss of function mutations of the *GJB2* gene detected in patients with DFNB1-associated hearing impairment. Neurobiol Dis 22:112–118

Richard G (2005) Connexin disorders of the skin. Clin Dermatol 23:23–32

Rivas MV, Jarvis ED, Morisaki S, Carbonaro H, Gottlieb AB, Krueger JG (1997) Identification of aberrantly regulated genes in diseased skin using the cDNA differential display technique. J Invest Dermatol 108:188–194

Snoeckx RL, Huygen PL, Feldmann D, et al. 2005. *GJB2* mutations and degree of hearing loss: a multicenter study. Am J Hum Genet 77:945–957

Stark HJ, Willhauck MJ, Mirancea N, Boehnke K, Nord I, Breitkreutz D, Pavesio A, Boukamp P, Fusenig NE (2004) Authentic fibroblast matrix in dermal equivalents normalises epidermal histogenesis and dermoepidermal junction in organotypic coculture. Eur J Cell Biol 83:631–645

Tran Van Nhieu G, Clair C, Bruzzone R, Mesnil M, Sansonetti P, Combettes L (2003) Connexin-dependent inter-cellular communication increases invasion and dissemination of shigella in epithelial cells. Nat Cell Biol 5:720–726

Wang HL, Chang WT, Li AH, Yeh TH, Wu CY, Chen MS, Huang PC (2003) Functional analysis of connexin–26 mutants associated with hereditary recessive deafness. J Neurochem 84:735–742

Wiszniewski L, Limat A, Saurat JH, Meda P, Salomon D (2000) Differential expression of connexins during stratification of human keratinocytes. J Invest Dermatol 115:278–285